ISBN: 978-3-95450-247-9 ISSN: 2673-5490 doi: 10.18429/JACoW-IPAC2024-THPS45

PROTON BEAM POWER LIMITS FOR STATIONARY WATER-COOLED TUNGSTEN TARGET WITH DIFFERENT CLADDING MATERIALS*

Y. Lee†, Oak Ridge National Laboratory, Oak Ridge, TN, USA

Abstract

The proton beam power limit for a solid-tungsten spallation target is largely determined by beam induced thermomechanical structural loads and decay heat power deposition, while its lifetime is limited by radiation damage and fatigue life of the target materials. In this paper, we studied the power limits of a stationary water-cooled solid tungsten target concept. Tantalum clad tungsten was considered as a reference case. Being a low activation material, zircaloy 2 cladding option was studied and its decay heat driven power limit was compared with the reference case. Zirconium alloys have proven operations records in spallation target and nuclear fission environments, supported by materials data obtained from post irradiation examinations. Recent study also demonstrated feasibility of diffusion bonding zirconium to tungsten using vanadium foil inter layer. Particle transport simulations code FLUKA was used to calculate energy deposition and decay heat power deposition in the target, based on the beam parameters technically feasible at the Second Target Station of the Spallation Neutron Source at Oak Ridge National Laboratory. The energy deposition data were used for flow, thermal, and structural analyses to determine the beam intensity limit on the target concept studied. The decay heat deposition data were used to calculate the transient temperature evolution in the tungsten volumes in a loss of coolant accident (LOCA) scenario to determine its beam power limit. For a 1.3 GeV proton beam, the power limit on a stationary target was 400 kW for a tantalum clad target model and 800 kW for a zircaloy 2 clad target model.

INTRODUCTION

Stationary water-cooled tantalum clad tungsten targets have served for leading spallation sources that include TS1 and TS2 at ISIS [1] and LANSCE at LANL [2] and CSNS [3]. Among them, the TS1 target at ISIS receives the highest beam power time averaged at 160 kW [4]. Tungsten targets for future spallation sources with higher proton beam powers adopted rotating target concepts. The European Spallation Source [5] and Second Target Station (STS) at Oak Ridge National Laboratory (ORNL) [6] will receive 5 MW and 0.7 MW beam power respectively. The rotating tungsten targets consist of dozens of target segments with the proton beam power uniformly distributed to each segment. This enable the target to handle a high beam power and grants longer lifetime with reduced number of fatigue cycles and radiation damage rate per each segment. Moreover, the rotating target has a large spallation volume that reduces the volumetric density of decay heat deposition. Its large surface area also enables efficient removal of the decay heat passively in loss of coolant accident (LOCA) cases. In LOCA, the surface temperature of tungsten shall not exceed 800 °C above which tungsten aggressively oxidizes and become volatile posing inhalation safety hazards [7]. Despite its merits with rotating targets for high beam powers, there are design, engineering, and operational challenges as it consists of many moving parts. Therefore, it is important to know the proton beam power limit on the stationary water-cooled tungsten target to avoid engineering complications involved with rotating tungsten target designs when possible.

FLUKA MODEL

FLUKA [8–10] was used for the calculations of energy deposition and decay power deposition in the target. The target model for FLUKA simulations is shown in Fig. 1. The

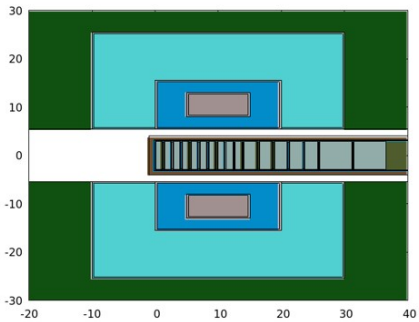

Figure 1: FLUKA geometry model used for energy deposition and decay heat calculations.

target consists of 17 tungsten bricks clad with 1 mm thick clad material. As clad materials, tantalum and zircaloy 2 were considered. The technical feasibility of hot isostatic pressing of zirconium alloys and tungsten utilizing vanadium foil inter layer to make zirconium alloy clad tungsten brick is demonstrated in Ref. [11]. These 17 bricks are welded together to have a monolithic structure like the new TS1 target at ISIS [4]. The height and width of the clad tungsten bricks are 60 mm and 200 mm respectively. The first ten bricks have a thickness of 12 mm, the next five bricks have a thickness of 22 mm, and each of the last two bricks is 52 mm thick. This arrangement provides total 300 mm net tungsten thickness which corresponds to the stopping range of a 1 GeV proton. These bricks are separated by 2 mm thin

† leey1@ornl.gov

ISBN: 978-3-95450-247-9 ISSN: 2673-5490 doi: 10.18429/JACoW-IPAC2024-THPS45

water channels to each other, which are connected to the main supply and return water ducts on the two sides of the 316L stainless steel vessel. The target is placed between the two cold neutron moderators that consist of water premoderator, cryogenic liquid hydrogen moderator and beryllium reflector. The dimensions of the presented target and moderator system is based on the current STS design.

For this study, a 1.3 GeV design beam energy for the STS at ORNL was used. A beam profile obtained from an STS beam dynamics study with a 60 cm^2 footprint on the target was used for the particle transport and thermal calculations.

BEAM POWER AND TARGET LIFETIME

Radiation Damage

It is important to keep the structural integrity of the target vessel made of 316L under radiation damage. At present, the administrative dose limit for the SNS target vessel made of 316L is 12 dpa to ensure the highest dose area of the target would retain at least 10% total elongation [12]. With 1.3 GeV proton beam with 60 cm^2 beam footprint on the target, the 12 dpa radiation damage in the beam entrance region can take up to 1.2 MW proton beam power for 5000 hours which is the annual beam-on time planned for STS.

Fatigue Life

The fatigue life of tungsten bricks mainly depends on beam spot size and its dimensions, for given pulse structure. To study the correlations among these parameters, we calculated steady and dynamic response of a tungsten brick to a design beam parameters on the STS target. Specifically, a 1.3 GeV proton beam with 700 kW beam power was used for the thermal and mechanical analyses. The STS beam has a repetition rate of 15 Hz and a pulse length of 0.7 μs. Two beam profiles were considered, a reference 60 cm^2 beam size and a 90 cm^2 beam size with a horizontally stretched reference beam configuration. The tungsten brick used for the study has a dimension of 200 mm (W) × 60 mm (H) × 10 mm (T). The beam facing surfaces are cooled by water with a wall heat transfer coefficient of 40 $kW{\cdot}m^{-2}{\cdot}K^{-1}$ for 300 K ambient temperature. This cooling efficiency can be achieved with a mass flow rate of 0.7 $kg{\cdot}s^{-1}$ per each water channel. A calculated energy deposition map in the third tungsten brick shown in Fig. 1, which has the highest energy deposition, was used for steady and transient thermal and structural analyses. Table 1 shows the calculated maximum temperature on the tungsten surfaces and maximum Goodman fatigue stress amplitude for the two beam profiles considered. ANSYS Multiphysics Software [13] was used for the simulations. For conservatism, temperature dependent thermal conductivity of irradiated tungsten was used [14]. Also shown is the fatigue factor of safety assuming 5000 hour operation at 700 kW beam power. The fatigue limit taken here is one third of the flexural strength of the irradiated tungsten reported in Ref. [15]. Note that the fatigue factor of safety is larger than 1.0 for the 90 cm^2 footprint, indicating that the tungsten brick could take 700 kW beam. To further increase the beam power limit on the target, either the beam footprint on the target should be enlarged or tungsten brick thickness be reduced.

Table 1: Fatigue Factor of Safety of a Tungsten Brick

Beam Size	**60 cm^2**	**90 cm^2**
Max. Surface Temperature	114.95 °C	85.32 °C
Max. Str. Amp. (Goodman)	273.43 MPa	99.42 MPa
Fatigue Limit	100 MPa	100 MPa
Factor of Safety	0.37	1.01

BEAM POWER AND DECAY HEAT

Decay Heat Power

Figure 2 shows a calculated decay power deposition at the end of 5000 hours of proton bombardment. The decay power density is higher in the beam stopping region. There are regions close to the moderators with a high decay heat deposition. This is largely due to thermal neutron capture by the cladding materials.

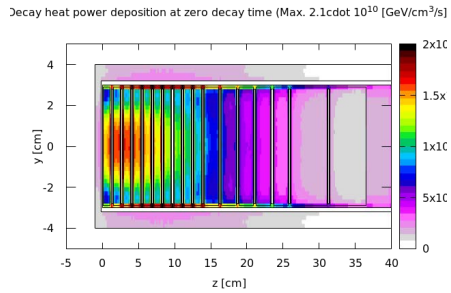

Figure 2: Calculated decay heat deposition configuration at the end of proton bombardment.

Table 2 shows the total decay heat at zero decay time, which are calculated for each material volume and normalized to 100 kW proton beam power. The decay heat for different cooling times are also calculated for transient thermal simulations. In calculating decay heat power depositions two different electron and gamma transport models were used. With EMF-ON, electrons and photons are transported

Table 2: Decay Heat at $t = 0$ per 100 kW Beam Power

Target		**EMF-OFF**	**EMF-ON**
Ta-Clad Target	W	383 W	478 W
	Ta	352 W	193 W
	SS-316L	41.7 W	53.0 W
Zr-Clad Target	W	429 W	448 W
	Zirc-2	57.0 W	22.6 W
	SS-316L	44.9 W	39.0 W

ISBN: 978-3-95450-247-9 ISSN: 2673-5490 doi: 10.18429/JACoW-IPAC2024-THPS45

and with EMF-OFF these particles are not transported. The EMF-OFF option resulted in higher decay power. Note that a low activation material cladding results in considerably lower decay power compared to tantalum cladding.

Recent study reported that the decay heat calculated with FLUKA with EMF-OFF card is up to 40% lower compared to MCNP6/CINDER2008 which does not transport electrons and photons [16] . A similar large difference between the FLUKA and MCNPX/CINDER90 was reported for a TS1 target at ISIS [17, 18]. A validation experiment with a TS1 target showed that its measured temperature data at different decay times agree well with the FLUKA predictions using the default EMF-ON [17]. Therefore, we assume that the FLUKA/EMF-OFF data provide a reasonable conservatism in decay power deposition estimates for this study.

Thermal and Flow Dynamics Model

ANSYS Multiphysics Software [13] was used for calculating temperature field of the target in a LOCA scenario. The geometry used for the calculation is shown in Fig. 3. The spallation volume consisting of tungsten bricks and stainless steel vessel are identical to the FLUKA model shown in Fig. 1. Added is the vertical duct volume which was used for studying the effect of natural convection on decay heat removal. The target vessel is surrounded by 10 mm thin air atmosphere that is confined by shielding and moderator vessel surfaces. For simplicity, the inner vessel wall that holds the clad tungsten volume is not modeled, and the passive heat transfer modes available between the tungsten and the outer vessel are radiation, conduction via air and convection.

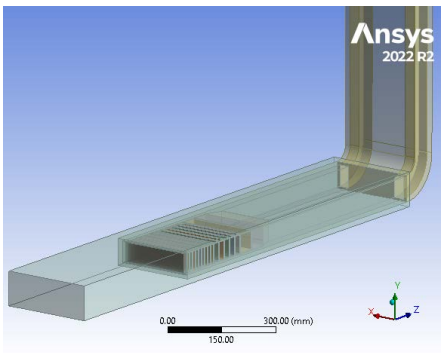

Figure 3: The geometry used for the temperature filed calculations.

In a LOCA situation, it is assumed that water is boiled out instantly and the coolant volume is completely replaced with air. For air, temperature dependent real gas data was used. Also assumed is complete instantaneous release of core vessel helium with atmospheric air replacing helium. Temperature dependent thermal and physical materials data were used for tungsten, tantalum, zircaloy 2 and stainless steel 316L. The moderator vessel made of aluminum 6061-T6 was not modeled. Instead, a low emissivity value of 0.05 was modeled on the surface area where the 10 mm thick air atmosphere faces the moderator. The shielding blocks were not modeled explicitly neither. Instead, the area where air atmosphere contacts surrounding shielding surface are modeled with constant temperature boundary condition at 400 K. This boundary condition is justified by the calculation presented in Ref. [19], which showed that the temperature on the shielding surface facing a 5 MW rotating tungsten target does not exceed 400 K in LOCA. For radiation heat transfer, a Discrete Ordinate Method was used with 24 rays.

Decay Heat and Power Limit

Figure 4 shows the calculated relation between the proton beam power and decay heat driven maximum temperature in tungsten. The decay heat with EMF-Off yields higher maximum temperature in tungsten for given beam power. With the tantalum clad tungsten concept, the maximum temperature in tungsten exceeds 800 °C at slightly below 400 kW proton beam power, while the zircaloy 2 clad target exceeds this threshold temperature at about 750 kW. With EMF-ON, the power limits of the tantalum and zircalot 2 clad target options are about 450 kW and 800 kW. The power limit could be slightly increased by applying a high emissivity coating on the target vessel and shielding block surfaces. To study the effect of the surface blackening and natural convection, another set of calculations have been performed with buoyancy flow model and 0.8 total emissivity on the steel surfaces. The power limits on the tantalum and zircaloy 2 clad targets are then 400 kW and 800 kW respectively, using the more conservative EMF-OFF decay heat values.

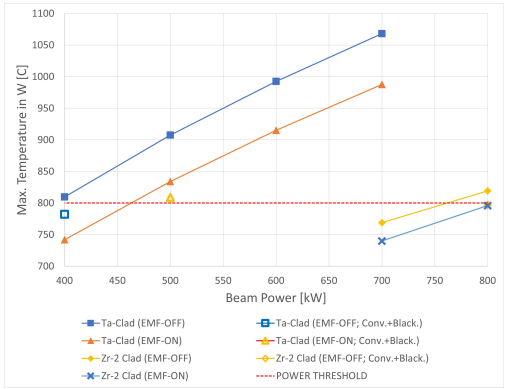

Figure 4: Calculated relation between the proton beam power and decay heat driven maximum temperature in tungsten.

CONCLUSIONS

With a tantalum clad water cooled tungsten target concept, the proton beam power limit was 400 kW for a 1.3 GeV proton kinetic energy. This power limit is constrained by its ability to passively remove decay heat in a LOCA case. The decay heat constrained power limit increases significantly with application of a low activation cladding material. In this paper zircaloy 2 was considered as alternative cladding material. The decay heat constrained power limit of the zircaloy 2 clad tungsten target was 800 kW.

ISBN: 978-3-95450-247-9 ISSN: 2673-5490 doi: 10.18429/JACoW-IPAC2024-THPS45

REFERENCES

[1] J. W. G. Thomason, "The ISIS Spallation Neutron and Muon Source—The first thirty-three years", *Nucl. Instrum. Methods Phys. Res., Sect. A*, vol. 917, pp. 61–67, Feb. 2019. doi:10.1016/j.nima.2018.11.129

[2] A. T. Nelson, J. A. O'Toole, R. A. Valicenti, and S. A. Maloy, "Fabrication of a tantalum-clad tungsten target for LANSCE", *J. Nucl. Mater.*, vol. 431, no. 1–3, pp. 172–184, Dec. 2012. doi:10.1016/j.jnucmat.2011.11.041

[3] S. Wei *et al.*, "Overview of CSNS tantalum cladded tungsten solid Target-1 and Target-2", *Nucl. Eng. Technol.*, vol. 54, no. 5, pp. 1535–1540, May 2022. doi:10.1016/j.net.2021.10.032

[4] L. G. Jones and D. Wilcox, "ISIS TS1 Project target – design for manufacture", *J. Phys. Conf. Ser.*, vol. 1021, p. 012056, May 2018. doi:10.1088/1742-6596/1021/1/012056

[5] R. Garoby *et al.*, "The European Spallation Source Design", *Phys. Scr.*, vol. 93, no. 1, p. 014001, Dec. 2017. doi:10.1088/1402-4896/aa9bff

[6] Oak Ridge National Laboratory, "Second Target Station Conceptual Design Report Volume 1: Overview, Technical and Experiment Systems", Rep. S01010000-TR0001 R00, Mar. 2020.

[7] G. A. Greene and C. C. Finfrock, "Vaporization of tungsten in flowing steam at high temperatures", *Exp. Therm Fluid Sci.*, vol. 25, no. 3–4, pp. 87–99, Oct. 2001. doi:10.1016/s0894-1777(01)00063-2

[8] G. Battistoni *et al.*, "Overview of the FLUKA code", *Ann. Nucl. Energy*, vol. 82, pp. 10–18, Aug. 2015. doi:10.1016/j.anucene.2014.11.007

[9] A. Ferrari *et al.*, "FLUKA: A Multi-Particle Transport Code", CERN, Rep. CERN-2005-010, 2005.

[10] V. Vlachoudis, "FFLAIR: A Powerful but User Friendly Graphical Interface for FLUKA", in *Proc. Int. Conf. on Mathematics, Computational Methods & Reactor Physics 2009*, Saratoga Springs, NY, USA, 2009, pp. 790–800.

[11] Y. J. Lee, J. Montross, J. Mach, and T. Muth, "Diffusion bonding of tungsten-vanadium-zirconium using vacuum hot pressing for the development of a low decay heat cladding solution for tungsten spallation targets", presented at the IPAC'24, Nashville, TN, USA, May 2024, paper THPS44, this conference.

[12] D. McClintock and B. Riemer, "Recommendation to Change the Region of Consideration for the SNS Target Administrative Dose Limit", Spallation Neutron Source(SNS), SNS Tech. Rep. 106010000-TR0130 R00, July 2015.

[13] ANSYS® Multiphysics Simulation Software, Release 2022 R2.

[14] J. Habainy, Y. Dai, Y. Lee, and S. Iyengar, "Thermal diffusivity of tungsten irradiated with protons up to 5.8 dpa", *J. Nucl. Mater.*, vol. 509, pp. 152–157, Oct. 2018. doi:10.1016/j.jnucmat.2018.06.041

[15] J. Habainy, Y. Dai, Y. Lee, and S. Iyengar, "Mechanical properties of tungsten irradiated with high-energy protons and spallation neutrons", *J. Nucl. Mater.*, vol. 514, pp. 189–195, Feb. 2019. doi:10.1016/j.jnucmat.2018.12.003

[16] Y. J. Lee and T. McClanahan, "Comparative study of decay heat calculations with FLUKA and MCNP/CINDER2008", presented at the IPAC'24, Nashville, TN, USA, May 2024, paper THPS43, this conference.

[17] L. Quintieri *et al.*, "Decay heat in ISIS spallation target: simulations and measurements", *J. Neutron Res.*, vol. 24, no. 3–4, pp. 313–327, Jan. 2023. doi:10.3233/jnr-220030

[18] L. Waters *et al.*, "The MCNPX Monte Carlo Radiation Transport Code", *AIP Conference Proceedings*, vol. 896, pp. 81–90, Mar.2007. doi:101063/12720459

[19] Y. Lee, "A new high power spallation target concept that works both for helium cooled and water cooled options", Tech. Rep. ESS-0463461, 2013.